# The Role of the Putative Inactivation Lid in Sodium Channel Gating Current Immobilization

Michael F. Sheets,* John W. Kyle,‡ and Dorothy A. Hanck§

From the *Nora Eccles Harrison Cardiovascular Research & Training Institute and The Department of Internal Medicine, University of Utah, Salt Lake City, Utah 84112; and ‡Department of Neurobiology, Pharmacology, and Physiology, and §Department of Medicine, University of Chicago, Chicago, Illinois 60637

abstract We investigated the contribution of the putative inactivation lid in voltage-gated sodium channels to gating charge immobilization (i.e., the slow return of gating charge during repolarization) by studying a lid-modified mutant of the human heart sodium channel (hH1a) that had the phenylalanine at position 1485 in the isoleucine, phenylalanine, and methionine (IFM) region of the domain III–IV linker mutated to a cysteine (ICM-hH1a). Residual fast inactivation of ICM-hH1a in fused tsA201 cells was abolished by intracellular perfusion with 2.5 mM 2-(trimethylammonium)ethyl methanethiosulfonate (MTSET). The time constants of gating current relaxations in response to step depolarizations and gating charge–voltage relationships were not different between wild-type hH1a and ICM-hH1a$_{MTSET}$. The time constant of the development of charge immobilization assayed at −180 mV after depolarization to 0 mV was similar to the time constant of inactivation of $I_{Na}$ at 0 mV for hH1a. By 44 ms, 53% of the gating charge during repolarization returned slowly; i.e., became immobilized. In ICM-hH1a$_{MTSET}$, immobilization occurred with a similar time course, although only 31% of gating charge upon repolarization (OFF charge) immobilized. After modification of hH1a and ICM-hH1a$_{MTSET}$ with Anthopleurin-A toxin, a site-3 peptide toxin that inhibits movement of the domain IV-S4, charge immobilization did not occur for conditioning durations up to 44 ms. OFF charge for both hH1a and ICM-hH1a$_{MTSET}$ modified with Anthopleurin-A toxin were similar in time course and in magnitude to the fast component of OFF charge in ICM-hH1a$_{MTSET}$ in control. We conclude that movement of domain IV-S4 is the rate-limiting step during repolarization, and it contributes to charge immobilization regardless of whether the inactivation lid is bound. Taken together with previous reports, these data also suggest that S4 in domain III contributes to charge immobilization only after binding of the inactivation lid.

key words: sodium channel • gating charge • inactivation • site-3 toxin • immobilization

## INTRODUCTION

The primary process by which voltage-gated sodium channels become nonconductive after opening in response to a strong step depolarization is called inactivation. Armstrong and Bezanilla (1977) were the first to demonstrate the relationship between fast inactivation of sodium ionic current ($I_{Na}$) and measurements of sodium channel gating currents ($I_g$), small asymmetrical currents that result from the movement of charged portions of the channel in response to changes in the electrical field. They showed that the time course of development of a slow component in $I_g$ recorded during repolarization at very negative potentials correlated with the time course of $I_{Na}$ inactivation. When the membrane potential was repolarized to less negative potentials, the slow component became too small and too slow to be accurately measured, and they described the gating charge as becoming "immobilized." Nearly 60% of the total sodium channel gating charge could become immobilized in squid giant axon, and similar values have been reported in other preparations (Meves and Vogel, 1977; Nonner, 1980; Starkus et al., 1981; Greeff et al., 1982).

Since the first cloning of a voltage-gated sodium channel by Noda et al. (1984), specific portions of the channel's sequence have become associated with specialized channel functions. The voltage sensors have been shown to reside, in large part, in the fourth transmembrane spanning segment (S4) in each of four domains that form the α subunit. Part of the fast inactivation process was localized to the intracellular region formed by the linker between domains III and IV by Vassilev et al. (1988), who used antibodies directed to this region and by Stühmer et al. (1989), who noted a prolongation of $I_{Na}$ decay when the linker was cut and channels expressed in two pieces. This intracellular linker has been called the "inactivation lid" after mutation of the three adjacent amino acids, isoleucine, phenylalanine, and methionine (IFM),[1] to QQQ

Portions of this work were previously published in abstract form (Sheets, M.F., J.W. Kyle, and D.A. Hanck. 2000. *Biophys. J.* 76:A193).

Address correspondence to Michael Sheets, M.D., CVRTI, Bldg. 500, 95 South 2000 East, University of Utah, Salt Lake City, UT 84112. Fax: 801-581-3128; E-mail: michael@cvrti.utah.edu

[1]*Abbreviations used in this paper:* Ap-A, Anthopleurin-A; hH1a, human heart sodium channel; ICM-hH1a, human heart sodium channel with F1485C mutation; IFM, isoleucine, phenylalanine, and methionine; MTSET, 2-(trimethylammonium)ethyl methanethiosulfonate; OFF charge, gating charge upon repolarization; ON charge, gating charge upon depolarization.

removed fast inactivation (see Fig. 1) in rat brain IIa (West et al., 1992) and in human heart (hH1a) (Hartmann et al., 1994). Additional studies have shown that the voltage sensor formed by domain IV–S4 has a unique role in channel inactivation (Chahine et al., 1994; Yang and Horn, 1995; Chen et al., 1996; Yang et al., 1996; Kontis et al., 1997; Kuhn and Greeff, 1999). In our previous studies, using a site-3 peptide toxin that binds to the outside of sodium channels (Rogers et al., 1996; Benzinger et al., 1998), we identified a component of sodium channel $I_g$ that is associated with inactivation from the open state (Hanck and Sheets, 1995; Sheets and Hanck, 1995), and we showed that the gating current component resulted from movement of the S4 in domain IV (Sheets et al., 1999). Recently, Cha et al. (1999), using site-directed fluorescent labeling of human skeletal muscle sodium channels, demonstrated that the S4 segments in domains III and IV, but not those in domains I and II, contributed to charge immobilization.

To investigate the role of the inactivation lid in charge immobilization, we studied the human cardiac sodium channel that had the phenylalanine at amino acid position 1485 in the IFM motif mutated to a cysteine (ICM-hH1a). The mutant sodium channel was transiently expressed in fused mammalian cells (Sheets et al., 1996), and the cysteine was modified by intracellular application of 2-(trimethylammonium)ethyl methanethiosulfonate (MTSET) to remove residual fast inactivation (ICM-hH1a$_{MTSET}$) (Kellenberger et al., 1996; Chahine et al., 1997; Vedantham and Cannon, 1998). Our results showed that the gating charge-voltage (Q-V) relationship and the dominant time constants of $I_g$ relaxations recorded during step depolarizations were unaltered regardless of whether the inactivation lid could bind to its receptor. In the absence of a functioning inactivation lid, charge immobilization still occurred in ICM-hH1a$_{MTSET}$ with a time course similar to that in wild-type hH1a, but only 31% of gating charge upon repolarization (OFF charge) became immobilized, compared with 53% in hH1a. Experiments with Anthopleurin-A (Ap-A) toxin, a site-3 toxin that inhibits movement of the S4 in domain IV, abolished charge immobilization for both hH1a and ICM-hH1a$_{MTSET}$. These data indicate that movement of the S4 in domain IV is the rate-limiting step in repolarization, and contributes to charge immobilization regardless of whether the inactivation lid is bound. Taken together with previous reports (Cha et al., 1999), these data also suggest that the S4 in domain III contributes to charge immobilization only after binding of the inactivation lid.

## METHODS

### *cDNA Clones*

In hH1a (kindly provided by H. Hartmann and A. Brown (see Hartmann et al., 1994) the phenylalanine in the IFM motif at amino acid position 1485 (Fig. 1) was mutated to a cysteine by four-primer PCR (Higuchi et al., 1988; Ho et al., 1989). The insert containing the mutated site was confirmed by sequencing. Because anecdotal evidence suggested that cell survival of inactivation-impaired mutants could be increased by blocking sodium channels during culturing, we increased the sensitivity of the ICM-hH1a channel to block by tetrodotoxin by mutating the cysteine at position 373 to a tyrosine (C373Y) (Satin et al., 1994; Chen et al., 1996). For expression of both hH1a and ICM-hH1a in mammalian cells, the cDNAs were subcloned directionally into the mammalian expression vector pRcCMV (Invitrogen Corp.).

### *Cell Preparation*

Multiple tsA201 cells (SV40-transformed HEK293 cells) or multiple HEK293 cells were fused together using polyethylene glycol, as previously described (Sheets et al., 1996). After fusion, the cells were placed in cell culture for several days to allow for membrane remodeling, and then they were transiently transfected using a calcium phosphate precipitation method (GIBCO BRL). For some experiments with wild-type hH1a, HEK293 cells that stably expressed hH1a were fused before transient transfection with cDNA coding for hH1a. ICM-hH1a expression appeared to be increased by the addition of 300 nM tetrodotoxin to the culture media 1 d after transfection. 3–6 d after transfection, fused cells were detached from culture dishes with trypsin-EDTA solution (GIBCO BRL) and studied electrophysiologically.

### *Recording Technique, Solutions, and Experimental Protocols*

Recordings were made using a large bore, double-barreled glass suction pipette for both voltage clamp and internal perfusion, as previously described (Hanck et al., 1990; Sheets et al., 1996). $I_{Na}$ was measured with a virtual ground amplifier (OPA-101; Burr-Brown) using a 2.5 MΩ feedback resistor. Voltage protocols were imposed from a 16-bit DA converter (Masscomp 5450; Concurrent Computer) over a 30/1 voltage divider. Data were filtered by the inherent response of the voltage-clamp circuit (corner frequency near 125 kHz) and recorded with a 16-bit AD converter on a Masscomp 5450 at 200 kHz. A fraction of the current was fed back to compensate for series resistance. Temperature was controlled using a Sensortek thermoelectric stage (TS-4; Physiotemp Instruments, Inc.) mounted beneath the bath chambers and it typically varied $<0.5$°C during an experimental set. Cells were usually studied at 12°–13°C.

A cell was placed in the aperture of the pipette and, after a high resistance seal formed, the cell membrane inside the pipette was disrupted with a manipulator-controlled platinum wire. Voltage control was assessed by evaluating the time course of the capacitive current and the steepness of the negative slope region of the peak current–voltage relationship as per criteria previously established (Hanck and Sheets, 1992). To allow for full sodium channel availability, the holding membrane potential was set to −150 mV. $I_g$ protocols typically contained four repetitions at each test voltage that were one fourth of a 60 Hz cycle out of phase to maximize rejection of this frequency and to improve the signal-to-noise ratio.

The control extracellular solution for $I_{Na}$ measurements contained (mM): 15 $Na^+$, 185 $TMA^+$, 2 $Ca^{2+}$, 200 $MES^-$, and 10 HEPES, pH 7.2; and the intracellular solution contained: 200 $TMA^+$, 200 $F^-$, 10 EGTA, and 10 HEPES, pH 7.2. For measurement of $I_g$, the intracellular solution contained (mM): 200 $TMA^+$, 50 mM $F^-$, 150 mM $MES^-$, 1 mM BAPTA (1,2-bis 2-aminophenoxy-ethane-*N*,*N*,*N′*,*N*-tetraacetic acid; Sigma Chemical Co.), 10 HEPES, and 10 EGTA, pH 7.2, 10 μM saxitoxin (Calbiochem Corp.), and the extracellular solution had $Na^+$ replaced with $TMA^+$. Reduction of intracellular $F^-$ and inclusion of BAPTA re-

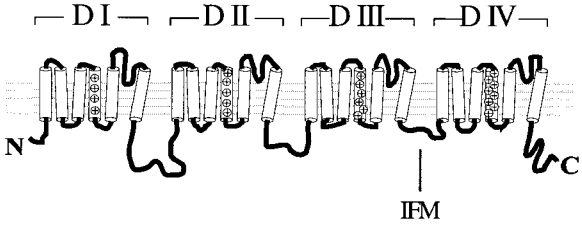


Figure 1. Predicted membrane topology of the sodium channel showing the four domains, each with six transmembrane segments, the charged residues in the fourth membrane–spanning regions (S4), and the intracellular locations of both the $NH_2$ and COOH termini. The phenylalanine at position 1485 in the IFM region of the linker between domains III and IV was mutated to a cysteine.

duced the magnitude of endogenous ionic currents that occasionally interfered with recordings. Anthopleurin A toxin (Sigma Chemical Co.) was used at a concentration of 1 μM, which is three orders of magnitude greater than the $K_d$ (Hanck and Sheets, 1995; Khera et al., 1995). For experiments in which cells were perfused internally with MTSET (Toronto Research Chemicals), it was dissolved in intracellular solutions ~1 min before use.

### *Data Analysis*

Leak resistance was calculated as the reciprocal of the linear conductance between −190 and −110 mV, and cell capacitance was measured from the integral of the current responses to voltage steps between −150 and −190 mV. Peak $I_{Na}$ was taken as the mean of four data samples clustered around the maximal value of data digitally filtered at 5 kHz and leak corrected by the amount of the calculated time-independent linear leak. Data were capacity corrected using 4–16 scaled current responses recorded from voltage steps between −150 and −190 mV. All $I_g$ were leak corrected by the mean of 2–4 ms of data, beginning at least 8 ms after the change in potential. For ON-$I_g$, this was typically at 8 ms, and 10 ms for OFF-$I_g$.

To determine time constants of $I_g$ decay, current traces were trimmed until the decay phase was clearly apparent, and then fit by a sum of exponentials with DISCRETE (Provencher, 1976), a program that provides a modified F statistic to evaluate the number of exponential components that best describe the data. To calculate the fraction of gating charge associated with each of the exponential components, it was necessary take into account the fact that the voltage clamp was not instantaneous. We first calculated the total OFF charge during each repolarization step, and then extrapolated the exponential curve backwards from the first point used for fitting until the total charge from the fitted curve equaled the total OFF charge for that voltage step. This method was a compromise between extrapolation of the data back to the start of the repolarization step, which would have resulted in over estimation of the contribution of the fast-time constant, and no extrapolation at all, which would have over estimated the contribution of the slow-time constant.

Charge-voltage relationships were fit with a simple Boltzmann distribution as follows:

$$Q = \frac{Q_{max}}{1 + e^{\frac{V_t - V_{1/2}}{s}}}, \quad (1)$$

where $Q$ is the charge during depolarizing step, $Q_{max}$ is the maximum charge, $V_t$ is the test potential, $V_{1/2}$ is the half point of the relationship, and $s$ is the slope factor in millivolts. For comparison between cells, fractional $Q$ was calculated as $Q/Q_{max}$ for each cell.

Data were analyzed and graphed on a SUN Sparcstation using SAS (Statistical Analysis System). Unless otherwise specified, summary statistics are expressed as means ± 1 SD. Regression parameters are reported as the estimate and the standard error of the estimate (S.E.E.), and figures show means ± SEM.

## RESULTS

### *Intracellular MTSET Modification of ICM-hH1a*

Similar to previous reports (Kellenberger et al., 1996; Chahine et al., 1997; Vedantham and Cannon, 1998), mutation of the phenylalanine to cysteine in the IFM motif in the linker between domains III and IV caused decay of $I_{Na}$ to be moderately slowed compared with wild-type hH1a, but perfusion with intracellular MTSET caused the decay to be almost completely inhibited (Fig. 2). We perfused cells expressing ICM-hH1a internally with 2.5 mM MTSET until additional slowing of the decay phase of $I_{Na}$ in response to step depolarizations was detectable (typically within 4 min), at which time the internal solution was changed back to control. Over the next 6 min, further modification occurred before decay of $I_{Na}$ stabilized with minimal inactivation over 50 ms (Fig. 2 C). As reported for other mammalian sodium channels (Yang and Horn, 1995; Kellenberger et al., 1996; Chahine et al., 1997), although not for squid giant axon (Khodakhah et al., 1998), internal perfusion with MTSET had no effect on $I_{Na}$ in wild-type hH1a ($n$ = 2, data not shown). In the following experiments, we compared $I_{Na}$ and $I_g$ measurements of ICM-hH1a$_{MTSET}$ to wild-type hH1a.

### *ON-Gating Current Studies*

If the putative inactivation lid were outside the voltage field and all voltage sensors had completed their translocation before the binding of the inactivation lid to its receptor, then $I_g$ measured during step depolarizations should be insensitive to whether the inactivation lid can become bound to its receptor. Fig. 3 shows capacity and leak-corrected $I_g$ traces and their corresponding integrals for typical cells expressing hH1a and ICM-hH1a$_{MTSET}$. $I_g$ decays were fit by a sum of up to two exponentials, and a two-time-constant fit was accepted when it produced a statistically significant F statistic (Provencher, 1976). The dominant time constant was assigned as the one making the larger contribution to total gating charge. For hH1a, two exponentials fit better 53% of the time, while for ICM-hH1a$_{MTSET}$ two exponentials fit better 77% of the time. When there was a second exponential, it contributed only 9% ± 8% ($n$ = 5) to the gating charge in hH1a and 15% ± 11% ($n$ = 4) to the charge in ICM-hH1a$_{MTSET}$ channels. There was no difference between the dominant time constants for the two channels at any of the test potentials (Fig. 3 C). In addition, the Q-V relationships were nearly identical between hH1a and ICM-hH1a$_{MTSET}$

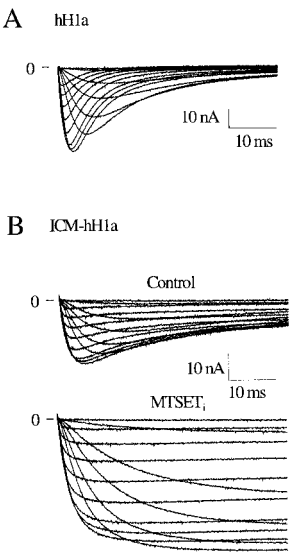


Figure 2. Families of leak and capacity-corrected $I_{Na}$ during step depolarizations to potentials between −120 and +40 mV from a holding potential of −150 mV for a cell expressing wild-type hH1a (A), and a cell expressing ICM-hH1a (B) in control (top) and after exposure to 2.5 mM intracellular MTSET (bottom). Cells Y4.02 and X5.02.

(Fig. 3 D). These data indicate that an intact putative inactivation lid did not directly contribute to gating charge upon depolarization (ON charge).

*Development of Ionic Current Inactivation of hH1a-ICM Sodium Channels after Intracellular MTSET*

A standard two-step development of inactivation protocol was used to assess the time course of fast inactivation of $I_{Na}$ (Fig. 4). Fig. 4 A (insert) illustrates the voltage-clamp protocol, which included a short voltage clamp-back step to −120 for 2 ms, which allowed any open sodium channels to close, but did not allow for recovery of inactivated channels. Over the 44-ms conditioning time, wild-type hH1a almost completely inactivated, while ICM-hH1a$_{MTSET}$ demonstrated little inactivation. Data for development times up to 1 s were fitted with the sum of two exponentials:

$$\text{Fractional Availability} = A_f e^{\frac{-t}{\tau_f}} + A_s e^{\frac{-t}{\tau_s}} + k, \qquad (2)$$

where the parameters determined by the fit were: $\tau_f$, the faster time constant, $A_f$, the amplitude contribution of $\tau_f$, $\tau_s$, the slower time constant, $A_s$, the amplitude contribution of $\tau_s$, and $k$ ($1 - A_f - A_s$), the noninactivating fraction, which was set to 0 for hH1a. Table I shows the values from fits to data from wild-type hH1a, ICM-hH1a$_{MTSET}$, and unmodified ICM-hH1a. For wild-type hH1a, the faster time constant was short (2.1 ± 0.3 ms) and accounted for most of the inactivation (83 ± 2%). In contrast, inactivation was almost completely abolished for ICM-hH1a$_{MTSET}$, with only 18% ± 2% ($n$ = 4) of the current inactivated by 44 ms, and the faster time constant (6.9 ± 3.0 ms) was more than three times longer than that for hH1a. Similar results were found when cells were perfused with 10 mM MTSET$_i$; only

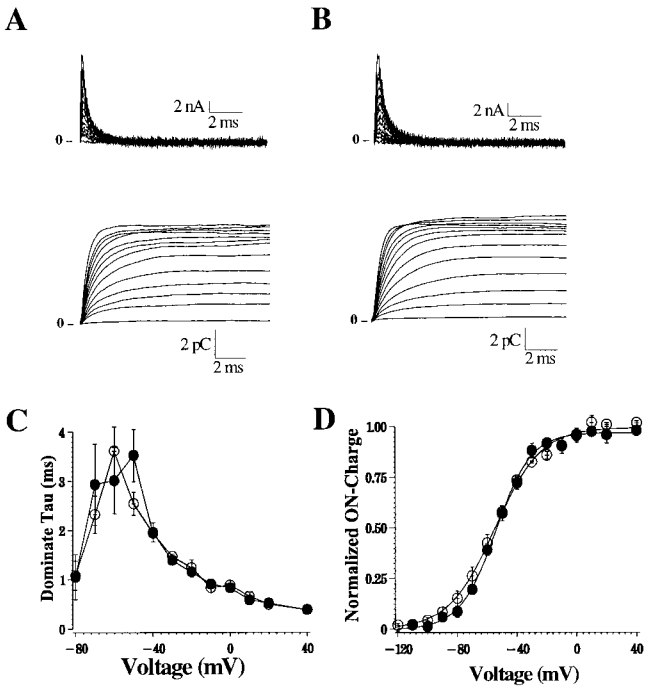


Figure 3. Family of gating currents (top) and their integrals (bottom) for typical fused cells expressing hH1a (A) and ICM-hH1a$_{MTSET}$ (B) for step depolarizations between −110 and +40 mV from a holding potential of −150 mV. Data are shown capacity and leak corrected, digitally filtered at 15 kHz, and with every fifth point plotted. (Cells Y3.03 and Y4.20.) (C) Voltage dependence of the dominant time constants (see text) obtained from fits to $I_g$ relaxations for five cells expressing hH1a channels (●) and for four cells expressing ICM-hH1a$_{MTSET}$ (○). (D) Q-V relationships for hH1a (●) and for ICM-hH1a$_{MTSET}$ (○). Data for each cell were normalized to their own $Q_{max}$. Solid lines represent the means of the best fits to each cell by a Boltzmann distribution (Eq. 1). The parameters from the best fits showed that, for hH1a ($n$ = 5 cells), the $V_{1/2}$ was −54 ± 4 mV, the slope factor was −12.0 ± 2.5 mV, and the mean $Q_{max}$ was 5.3 ± 2.8 pC; while, for ICM-hH1a$_{MTSET}$ ($n$ = 4 cells), the $V_{1/2}$ was −55 ± 4 mV with a slope factor of −15.5 ± 2.4 mV, and the mean $Q_{max}$ was 8.9 ± 3.8 pC.

16% ± 6% ($n$ = 4) of the current inactivated by 44 ms (data not shown). The residual "fast" inactivation in ICM-hH1a$_{MTSET}$ was unlikely to reflect residual ICM-hH1a unmodified by MTSET$_i$ because the fast time constant of unmodified ICM-hH1a was much shorter (1.4 ± 0.3 ms). In addition, although a second time constant was present for each channel isoform, the slow time constant for ICM-hH1a$_{MTSET}$ would contribute little to the small reduction in $I_{Na}$ at 44 ms because it was nearly 80-fold longer than the fast time constant.

*OFF-gating Current Studies*

To investigate the contribution of the putative inactivation lid to gating charge immobilization (i.e., the slow return of gating charge during repolarization), $I_g$ was recorded during repolarization steps to −180 mV after conditioning to 0 mV for up to 44 ms in cells express-

TABLE I

*Comparison of Parameters from Two Exponential Fits to the Development of $I_{Na}$ Inactivation (see Fig. 4)*

| Na channel | *n* | Fast tau | Amplitude of fast tau | Slow tau | Amplitude of slow tau | Constant |
|---|---|---|---|---|---|---|
| | | *ms* | *fraction* | *ms* | *fraction* | *fraction* |
| hH1a | 7 | 2.1 ± 0.3 | 0.83 ± 0.02 | 21.7 ± 10.9 | 0.17 ± 0.02 | 0 |
| ICM-hH1a$_{MTSET}$ | 4 | 6.9 ± 3.0 | 0.12 ± 0.03 | 406 ± 158 | 0.43 ± 0.14 | 0.46 ± 0.14 |
| ICM-hH1a | 6 | 1.4 ± 0.3 | 0.50 ± 0.06 | 59 ± 22 | 0.24 ± 0.03 | 0.26 ± 0.04 |

ing wild-type hH1a and ICM-hH1a$_{MTSET}$. The potential of −180 mV was selected for recording of $I_g$ during repolarization (OFF-$I_g$) because the slow component became fast enough such that all of the OFF charge could be measured over 10–15 ms (i.e., the OFF charge measurement equaled the ON charge measurement), but it was still long enough that the slow and fast time constants of OFF-$I_g$ were different by about an order of magnitude and could be clearly separated using two exponential fits. Examples of OFF-$I_g$ and their integrals are shown for hH1a and ICM-hH1a$_{MTSET}$ in Fig. 5. The presence of a slow component is more apparent by inspection of the integrals of OFF-$I_g$ (bottom).

OFF-$I_g$ were fit by a sum of up to two exponentials, and the time constants sorted by speed. Fig. 6 shows the results of this analysis for both hH1a and ICM-hH1a$_{MTSET}$. For this and subsequent experiments, results from five cells expressing hH1a were compared with those from four cells expressing ICM-hH1a$_{MTSET}$. The values for both $\tau_f$ and $\tau_s$ were very similar for the two groups with a faster time constant of $<$0.4 ms and a slower time constant of $\sim$2 ms. Note that no slow time constant was detectable until the duration of the conditioning step was at least 0.7 ms for either channel type.

Even though the time constants of relaxations of OFF-$I_g$ traces for hH1a and ICM-hH1a$_{MTSET}$ were similar, the contributions to OFF charge were very different between the two channels (Fig. 7). Data are graphed in a manner similar to those presented by Armstrong and Bezanilla (1977), who first showed that the time course in the reduction of the fast component in OFF charge was the same as the time course of development of $I_{Na}$ inactivation. Because the sum of the charge in the fast- and slow-time constants equals unity, the time course of appearance of a slow component in OFF charge is equivalent to the time course of reduction in the contribution by the fast component. The fraction of OFF charge accounted for by the fast component calculated for each development duration compared with the total OFF charge measured for the same development duration for wild-type hH1a and ICM-hH1a$_{MTSET}$ is shown in Fig. 7. With the shortest conditioning duration of 0.3 ms, all of the OFF charge was accounted for in the fast component, but, as the conditioning duration was extended, the fast component accounted for a smaller fraction of the OFF charge.

For hH1a, the fraction of OFF charge contributed by the fast-time constant decreased with a time constant of 2.8 ± 2.3 ms, which was similar to the time course of the development of $I_{Na}$ inactivation at 0 mV (2.1 ms, Table I). It reached a steady state value of 47 ± 10%, where the slow component accounted for the remainder (53%) of the total OFF charge. Surprisingly, in the absence of a normally functioning inactivation gate (i.e.,

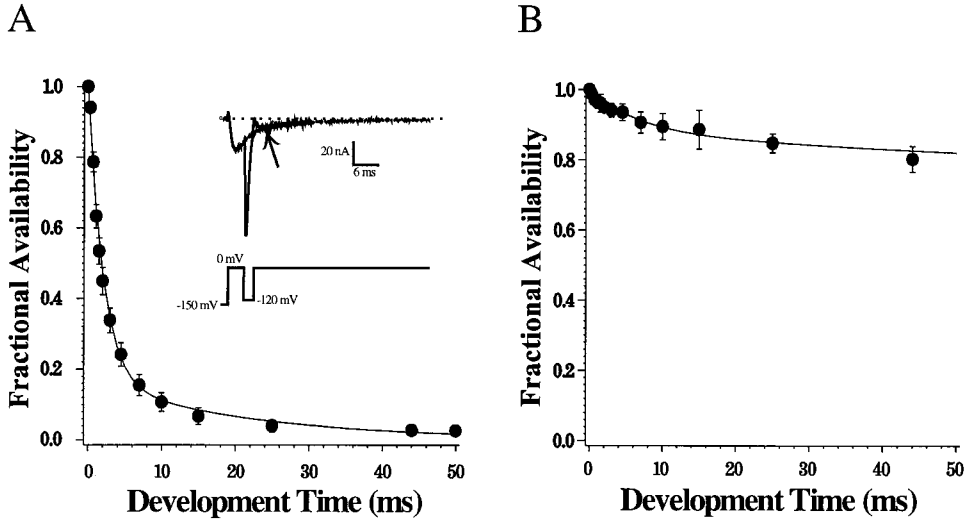


Figure 4. Two-pulse development of $I_{Na}$ inactivation for wild-type hH1a (A) and ICM-hH1a$_{MTSET}$ (B). The inset illustrates the voltage-clamp protocol and an example of a capacity and leak-corrected $I_{Na}$ trace from a cell expressing hH1a. Peak $I_{Na}$ after various conditioning times to 0 mV were normalized to the peak $I_{Na}$ in the absence of a conditioning step for each cell. The solid lines were calculated from the means of the parameters of the individual fits to Eq. 2. Fitted parameters are given in Table I.

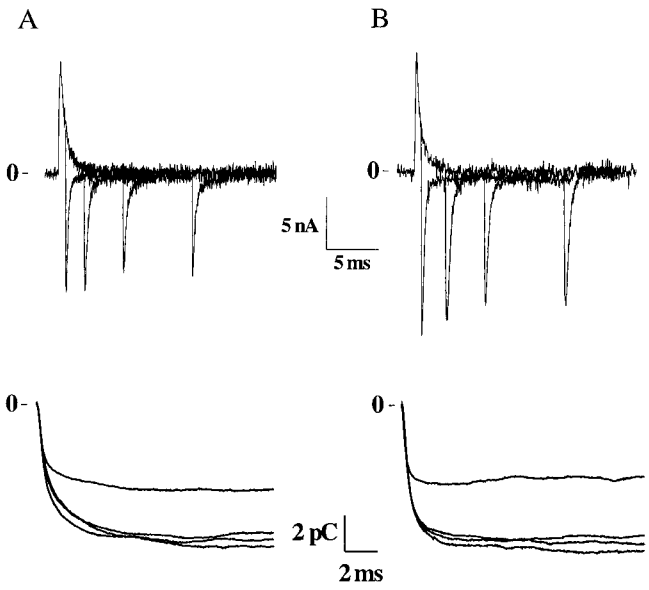


Figure 5. OFF-gating currents (top) and their integrals (bottom) recorded during repolarization to −180 mV after conditioning steps to 0 mV for 0.7, 3, 7, and 15 ms for hH1a (A) and ICM-hH1a$_{MTSET}$ (B). Also shown for each cell is the ON-$I_g$ in response to a step depolarization to 0 mV from a holding potential of −150 mV. Data are shown capacity and leak corrected, digitally filtered at 15 kHz, and with every fourth point plotted. (Cells Y3.03 and Y4.40.)

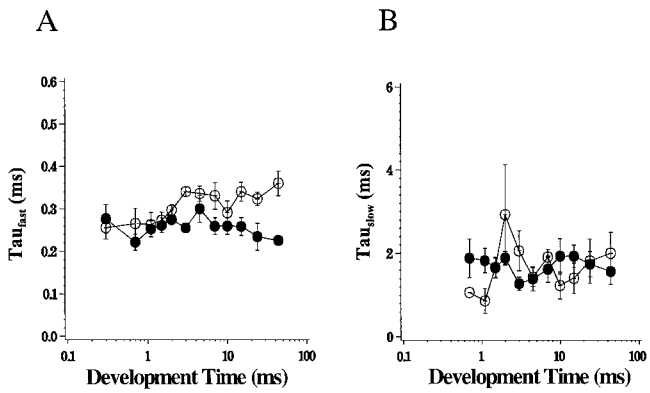


Figure 6. Time constants of OFF-gating current relaxations during repolarization to −180 mV after conditioning to 0 mV for 0.3–44 ms. The holding potential was −150 mV. Fast (A) and slow (B) time constants obtained from fits to Eq. 2 for cells expressing wild-type hH1a (●) and ICM-hH1a$_{MTSET}$ (○). Time constants were similar except those at times longer than 10 ms, which tended to increase slightly in ICM-hH1a$_{MTSET}$.

in ICM-hH1a$_{MTSET}$), there still remained two time constants in OFF-$I_g$. The time course of the decrease in the fraction of OFF charge accounted by the fast-time constant had a similar value (2.5 ± 1.4 ms) to that for hH1a, although the fraction of OFF charge that was accounted for by the fast-time constant after longer conditioning durations was 69 ± 9%, while the fraction of OFF charge accounted for by the slow component decreased to 31% ($P < 0.01$ compared with wild-type hH1a by non-paired $t$ test). Analysis of the time course of the appearance of the slow component in the OFF charge gave nearly equivalent values; time constants and amplitudes were 2.1 ± 1.9 ms and 52 ± 10% (wild-type hH1a) and 3.6 ± 3.0 ms and 33 ± 3% (ICM-hH1a$_{MTSET}$). In one cell, we confirmed that wild-type hH1a perfused with intracellular MTSET showed no changes in OFF-$I_g$.

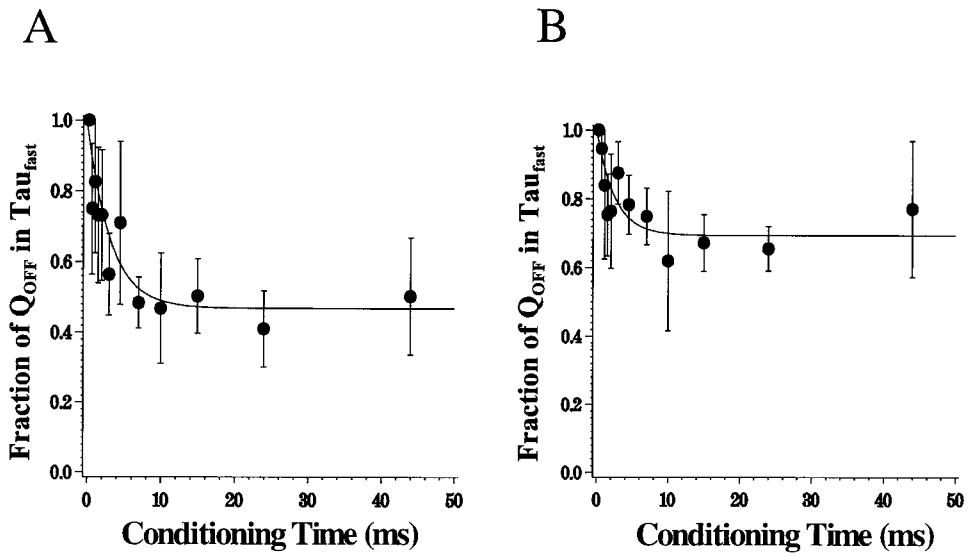


Figure 7. Fraction of OFF charge associated with the fast-time constant for hH1a (A) and ICM-hH1a$_{MTSET}$ (B), normalized to the total OFF charge measured during the same repolarization step. Voltage-clamp protocols and cells were the same as in Fig. 6. The solid lines were calculated from the means of the parameters from single exponential fits to the data for each cell according to Eq. 3.

$$\frac{Q_f}{Q_{OFF}} = (1 - A_f)e^{\frac{-t}{\tau_Q}} + A_f, \quad (3)$$

where fractional charge was calculated as the ratio of charge associated with the faster time constant ($Q_f$) to the total OFF charge at each time, and the parameters determined by the fit were: $\tau_Q$, the time constant of the reduction in the contribution to OFF charge by the fast time constant, and $A_f$, the steady state amplitude of OFF charge associated with the fast time constant while $1 - A_f$ represents the steady state amplitude of the OFF charge associated with the slow-time constant. The parameters from the best fits for hH1a ($n = 5$ cells) showed that $\tau_Q$ was 2.8 ± 2.3 ms; $A_f$, the fraction of OFF charge in the fast tau, was 0.47 ± 0.10; and $1 - A_f$, the fraction of OFF charge in the slow tau, was 0.53 ± 0.10.* For ICM-hH1a$_{MTSET}$ ($n = 4$ cells), $\tau_Q$ was 2.5 ± 1.4 ms, $A_f$ was 0.69 ± 0.09, and $1 - A_f$ was 0.30 ± 0.09.* *$P < 0.01$.

While it is possible that the slow-time constant in ICM-hH1a$_{MTSET}$ was related to residual inactivation of unmodified channels, this seems unlikely for the following reasons. First, the fast-time constant of $I_{Na}$ inactivation in ICM-hH1a$_{MTSET}$ was more than threefold longer than that in unmodified ICM-hH1a channels (6.9 vs. 1.4 ms, see Table I). Second, if inactivation of residual, non–MTSET-modified ICM-hH1a channels were responsible for the fast-time constant that remained in the OFF charge, then the amount of OFF charge accounting for the slow component should have been much smaller than the measured 31%. After all wild-type hH1a channels have been fast inactivated, ~47% of the OFF charge returned rapidly and 53% returned slowly. Applying a similar ratio to OFF charge of ICM-hH1a$_{MTSET}$, where <20% of $I_{Na}$ became inactivated by 44 ms (Fig. 4), it would be expected that <10% of the charge should have become immobilized. Instead, >30% of the charge was contained in the slow-time constant. Lastly, the time constant of $I_{Na}$ inactivation at 0 mV for ICM-hH1a$_{MTSET}$ (6.9 ms) did not correspond to its time constant of development of immobilization (2.5 ms). Consequently, it is more likely that one or more of the four putative voltage sensors of ICM-hH1a$_{MTSET}$ return to their repolarized conformation with a slow-time constant even in the absence of an intact inactivation lid.

*The Effect of Inhibition of Movement of the Domain IV–S4 on Charge Immobilization*

We have shown that Ap-A toxin slows inactivation of $I_{Na}$ by inhibiting movement of the voltage sensor formed by the S4 of domain IV (Hanck and Sheets, 1995; Sheets et al., 1999). We postulated, therefore, that this toxin could be used to probe the contribution of the S4 in domain IV to the slow component of OFF charge in the lid-modified mutant.

Because fast inactivation had already been modified in ICM-hH1a$_{MTSET}$ cells, the application of Ap-A toxin had little additional effect on $I_{Na}$ decay (data not shown). However, because Ap-A toxin also reduces $Q_{max}$ by about one-third (Sheets and Hanck, 1995, 1999), the Q-V relationship could be used to verify that channel modification by toxin had occurred. Fig. 8 shows that Ap-A toxin reduced $Q_{max}$ by about one-third in both wild-type hH1a and ICM-hH1a$_{MTSET}$. Furthermore, the slope factors and half-points of the Q-V relationships for the two channels were comparable. The reduction in $Q_{max}$ by Ap-A toxin in ICM-hH1a$_{MTSET}$ confirmed that the toxin still modified ICM-hH1a$_{MTSET}$ ON charge similar to wild-type hH1a, even though inactivation of $I_{Na}$ had already been slowed.

The role of the domain IV–S4 in charge immobilization was then investigated by recording OFF-$I_g$ for both hH1a and ICM-hH1a$_{MTSET}$ after modification by Ap-A toxin. The same voltage protocol was used as previously; cells were depolarized to 0 mV for durations up to 44 ms before repolarization to −180 mV. OFF-$I_g$ were fit by a sum of up to two exponentials and sorted by speed. In contrast to the findings in control solutions (Fig. 6), OFF-$I_g$ for both hH1a and ICM-hH1a$_{MTSET}$ were best fit by a single exponential at all conditioning durations (Fig. 9). The time constants clustered around 0.3 ms, and they were similar to the fast-time constants recorded for both hH1a and ICM-hH1a$_{MTSET}$ cells in control solutions (Fig. 6 A). A decrease in the amount of charge immobilization has been previously reported in frog myelinated nerve after exposure to site-3 toxins (Neumcke et al., 1985).

To compare the magnitude of OFF charge for the two channels after toxin modification, the fraction of OFF charge in Ap-A toxin was normalized to the maximal OFF charge (i.e., $Q_{max}$) measured for each cell in the absence of toxin and plotted as a function of the duration of the conditioning pulse at 0 mV. These data are shown in Fig. 10 A for both wild-type hH1a and ICM-hH1a$_{MTSET}$. The time course of the increase in OFF charge was nearly identical for both sodium channels with a time constant of ~0.7 ms. Note that the largest fraction of OFF charge was almost 70%, consistent with the reduction in gating charge by Ap-A toxin (Fig. 9). Both the absence of a slow component in the OFF

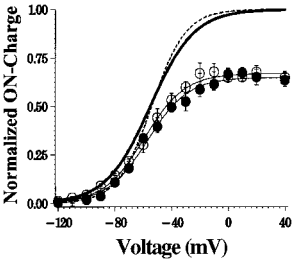


Figure 8. Effects of Ap-A toxin on ON charge. Q-V relationships for hH1a (●) and ICM-hH1a$_{MTSET}$ (○) after modification by 1 μM Ap-A toxin. ON charge was normalized to the $Q_{max}$ in control solution for each cell. The dashed line and thick line represent the fits to the Q-V relationships for hH1a and ICM-hH1a$_{MTSET}$ in control solutions, respectively, from Fig. 3. The thin solid lines represent the mean of the best fits to each cell by a Boltzmann distribution (Eq. 1). The parameters from the best fits showed that for hH1a ($n$ = 5 cells), the $V_{1/2}$ was −57 ± 5 mV, the slope factor was −14.3 ± 2.9 mV, and the mean normalized $Q_{max}$ was 0.62 ± 0.07 pC, while for ICM-hH1a$_{MTSET}$ ($n$ = 4 cells), the $V_{1/2}$ was −59 ± 4 mV, with a slope factor of −14.3 ± 3.0 mV, and the mean normalized $Q_{max}$ was 0.67 ± 0.09 pC.

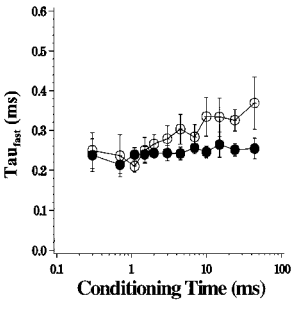


Figure 9. Time constants of OFF-gating currents after modification by Ap-A toxin for cells expressing wild-type hH1a (●) and ICM-hH1a$_{MTSET}$ (○). Voltage protocol and data analysis were the same as in Fig. 6. In contrast to the control condition, all OFF-$I_g$ were best fit by a single exponential. Note the similar values to the very fast-time constant obtained in the absence of toxin (Fig. 6 A).

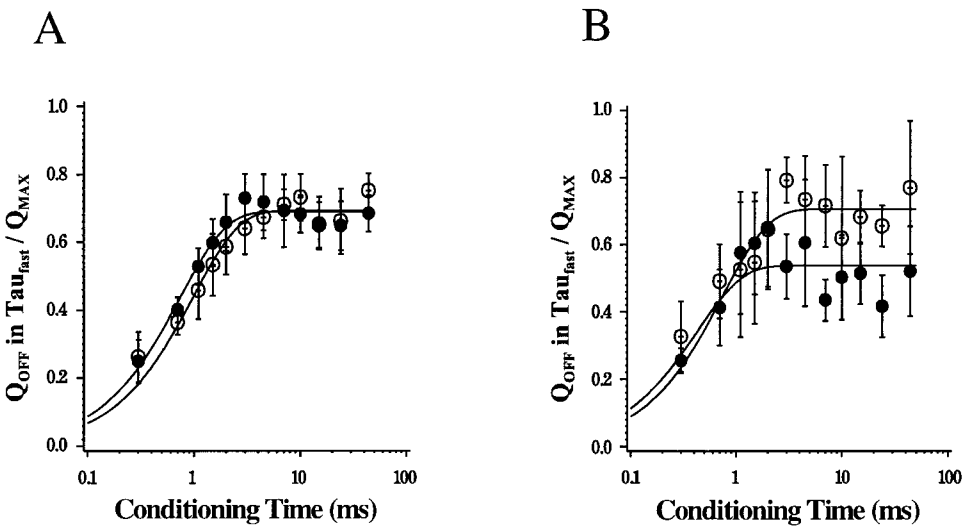


Figure 10. Fraction of OFF charge normalized to the cell's maximal OFF charge in control after a conditioning step to 0 mV for durations up to 44 ms. Solid lines were calculated using the means of fitted parameters from each cell to the following:

$$\text{fractional } Q = A\left(1 - e^{\frac{-t}{\tau}}\right), \quad (4)$$

where the parameters of the fit were the time constant ($\tau$) of the appearance of OFF charge and *A*, the fractional amplitude returned. (A) Fractional Q was calculated as the ratio of OFF charge at the times indicated in Ap-A toxin to the maximal OFF charge in control solutions for hH1a (●) and ICM-hH1a$_{MTSET}$ (○). (B) Fractional Q was calculated as the ratio of OFF charge in the fast time constant at the times indicated in control solutions (see Fig. 7) to the maximal OFF charge in control for hH1a (●) and ICM-hH1a$_{MTSET}$ (○). Note that both the amplitude and time course of OFF charge associated with the fast time constant for ICM-hH1a$_{MTSET}$ were comparable with those of both toxin-modified channels. The parameters from the best fits are given in Table II.

charge of ICM-hH1a$_{MTSET}$ after toxin modification and the ~30% reduction in OFF charge suggest that the slow component of OFF charge for ICM-hH1a$_{MTSET}$ in control solutions (Fig. 7) may result from the slow return of charge associated with the S4 in domain IV.

If this were the case, then one would expect the OFF charge associated with the fast-time constant in ICM-hH1a$_{MTSET}$ to be similar to the OFF charge of both toxin-modified ICM-hH1a$_{MTSET}$ and toxin-modified wild-type hH1a. Fig. 10 B shows the time course of the appearance of OFF charge contributed by the fast time constant in control solutions for both wild-type hH1a and ICM-hH1a$_{MTSET}$ normalized to maximal OFF charge (i.e., $Q_{max}$). Note that the fraction and time course of OFF charge contributed by the fast-time constant in ICM-hH1a$_{MTSET}$ recorded in control solutions was nearly identical to that for toxin-modified ICM-hH1a$_{MTSET}$. Also shown in Fig. 10 B is the time course and magnitude of the fraction of OFF charge accounted for by the fast component for wild-type hH1a recorded in control solutions.

## DISCUSSION

To study the role of putative inactivation lid on charge immobilization, we investigated hH1a that had the phenylalanine at position 1485 in the IFM region of the domain III–IV linker mutated to a cysteine (F1485C). Although the mutation itself has been shown to only moderately disrupt $I_{Na}$ inactivation in three different mammalian sodium channel isoforms (rat brain IIa, skeletal muscle, and heart), fast inactivation is almost completely eliminated by exposure of the mutated cysteine to intracellular MTSET (Kellenberger et al., 1996; Chahine et al., 1997; Vedantham and Cannon, 1998). We used this approach to study the contribution of binding of the inactivation lid to gating charge immobilization in fused mammalian cells expressing ICM-hH1a. Al-

TABLE II

*Parameters from Fits to Eq. 4 for Fraction of OFF Charge Normalized to Maximal OFF Charge in Control*

| Na channel isoform | *n* | Toxin present | A (fractional amplitude) | Tau |
|---|---|---|---|---|
| | | | | *ms* |
| hH1a | 5 | yes | 0.69 ± 0.08 | 0.74 ± 0.15 |
| ICM-hH1a$_{MTSET}$ | 4 | yes | 0.69 ± 0.06 | 0.98 ± 0.17 |
| Fast component in ICM-hH1a$_{MTSET}$ | 4 | no | 0.71 ± 0.09 | 0.74 ± 0.24 |
| Fast component in hH1a | 5 | no | 0.54 ± 0.07 | 0.42 ± 0.10 |

There was no significant difference ($P < 0.05$) between the amplitudes and taus of OFF charge for ICM-hH1a$_{MTSET}$ in toxin and either wild-type hH1a in toxin or OFF charge associated with the fast time constant of ICM-hH1a$_{MTSET}$ in control solution.

though fast inactivation had been modified in this preparation, inactivation over hundreds of milliseconds can still occur in sodium channels with mutations in the IFM motif (Featherstone et al., 1996). Such slow inactivation was not addressed in the studies reported here.

We found that the Q-V relationships of wild-type hH1a and ICM-hH1a$_{MTSET}$ were similar, as were the time courses of ON-$I_g$ relaxations, demonstrating that an intact inactivation lid had little effect on movement of the channel's voltage sensors during step depolarizations. However, comparison of the OFF-charge measurements between the two sodium channels showed that 53% of the charge became immobilized in wild-type hH1a, while only 31% of the charge became immobilized in ICM-hH1a$_{MTSET}$. After the application of Ap-A toxin, a site-3 peptide toxin that has been shown to modify inactivation of $I_{Na}$ by inhibiting movement of the S4 segment of domain IV (Sheets et al., 1999), the OFF charge was similar in both magnitude and time course for both wild-type hH1a and ICM-hH1a$_{MTSET}$.

*The Role of the Inactivation Lid in Charge Immobilization*

Armstrong and Bezanilla (1977) found that the OFF charge of inactivated sodium channels in squid giant axon contained two components, a fast and a slow component, with the slow component (immobilizable fraction) accounting for nearly 60% of the total charge. Furthermore, the time course of the reduction in the fast component in OFF charge (as well as the time course of the development of the slow component) paralleled the time course of development of $I_{Na}$ inactivation. When the repolarization voltage was less negative, the slow component of the OFF charge was too small and too slow to be accurately measured. As a consequence, the magnitude of the OFF charge was reduced compared with ON charge, and the gating charge was said to become immobilized. We found a similar correlation between the time course of reduction in the fast component of OFF charge and the degree of inactivation of $I_{Na}$. In wild-type hH1a, the predominant time constant of $I_{Na}$ inactivation at 0 mV was 2.1 ms, which was comparable with both the time course of reduction in the fast component (2.8 ms) and to the appearance of the slow component (2.1 ms) in OFF charge (Figs. 4 and 7). After longer conditioning durations, the slow component accounted for up to 53% of total OFF charge, similar to the nearly 60% found for sodium channels in squid giant axon (Armstrong and Bezanilla, 1977; Greeff et al., 1982) and to the 56% found for heterologously expressed rat brain IIa (Kuhn and Greeff, 1999).

Armstrong and Bezanilla (1977) also found that internal perfusion of the squid giant axon with the nonspecific proteolytic enzyme, pronase, removed both fast inactivation and charge immobilization. Based on this finding, it seemed reasonable to expect that focal disruption of the putative inactivation lid of sodium channels might also eliminate charge immobilization. However, we found that was not the case; the amount of OFF charge in ICM-hH1a$_{MTSET}$ that could become immobilized was reduced but not eliminated (from 53% to 31%). In ICM-hH1a$_{MTSET}$, charge immobilization still occurred with a time course of 2.5 ms (Fig. 7), which was similar to the time course in wild-type hH1a. Although fast inactivation was "removed" by either intracellular proteolytic enzymes or by mutagenesis, these results suggest that the two methods are not equivalent. Similarly, differences between the two methods has been shown for cardiac Na channels where modification of fast inactivation by proteolytic enzymes enhanced slow inactivation (Clarkson, 1990), whereas mutation of the inactivation lid had little effect on slow inactivation (Bennett et al., 1995). Because proteolytic enzymes are expected to cleave the Na channel protein at multiple sites, it is likely that intracellular proteolytic enzymes produce more complicated channel modifications than that achieved by channel mutagenesis. Consequently, differing effects on movement of the voltage sensors would not be unexpected.

In the absence of binding of the inactivation lid, what then is the origin of the gating charge that can become immobilized in ICM-hH1a$_{MTSET}$? Fig. 10 suggests that the S4 in domain IV is responsible for charge immobilization in ICM-hH1a$_{MTSET}$. Previous studies have shown that site-3 toxins such as Ap-A toxin bind extracellularly to regions in domain IV (Thomsen and Catterall, 1989; Rogers et al., 1996; Benzinger et al., 1997, 1998), and that site-3 toxins inhibit movement of the S4 of domain IV (Sheets and Hanck, 1995; Sheets et al., 1999). Consequently, sodium channels that are modified by Ap-A toxin allow only the S4s in domains I–III to contribute to gating charge. In Ap-A toxin, the time course and the magnitude of OFF charge for both wild-type hH1a and ICM-hH1a$_{MTSET}$ were the same (Fig. 10 A). Comparison of these data to the OFF charge associated with only the fast-time constant in ICM-hH1a$_{MTSET}$ in control solutions showed the time courses and magnitudes of the OFF charge to be analogous (Fig. 10 B), and suggests that the S4s in domains I–III in nontoxin-modified ICM-hH1a$_{MTSET}$ contributed to the fast component of OFF charge. Consequently, the S4 in domain IV appears to be responsible for the slow component of OFF charge in ICM-hH1a$_{MTSET}$.

These data also suggest that charge movement from the S4 in domain IV occurs on a slower time scale than activation. In the presence of Ap-A toxin, all OFF charge is contained in the fast component with a time course of appearance of $\sim$0.7 ms (Fig. 10), and represents the return of gating charge associated only with channel activation because fast inactivation has been inhibited

by the toxin. Similarly, because the fast component of OFF charge in ICM-hH1a$_{MTSET}$ is nearly identical to the OFF charge in Ap-A toxin, it also is likely to represent gating charge associated with channel activation resulting from movement of the S4s in domains I–III. The time course of appearance of the slow component of OFF charge in ICM-hH1a$_{MTSET}$ is much longer ($\sim$2.5 vs. 0.7 ms), suggesting that the S4 in domain IV moved after the other S4s had moved. This conclusion is consistent with previous ON charge studies showing that the S4 in domain IV moved after sodium channel activation had occurred (Sheets and Hanck, 1995; Sheets et al., 1999) and that it moved more slowly than the other S4s in domains I–III (Cha et al., 1999).

As shown in Fig. 7, there was an additional 22% of OFF charge in control solutions that returned slowly in wild-type hH1a (53%) compared with the amount that returned slowly in ICM-hH1a$_{MTSET}$ (31%). The data with Ap-A toxin suggest that this voltage sensor is not the S4 in domain IV, but they do not directly address what additional voltages sensors may be responsible for the slow return of OFF charge in wild-type hH1a. Recently, Cha et al. (1999) showed that charge immobilization was the result of slow movement of the S4 in domain III and even slower movement of the S4 in domain IV, while the voltage sensors from domains I and II returned rapidly and accounted for the fast component of OFF charge that did not immobilize. Our results are consistent with these data and suggest that the S4 in domain III is the voltage sensor responsible for contributing an additional component to the OFF charge that returns slowly only when the inactivation lid has bound. Interestingly, residues in the S4–S5 linker in domain III have been implicated as forming part of the inactivation lid receptor site (Smith and Goldin, 1997).

### *Implications for a Structurally Based Model*

The experiments reported here expand upon the model recently proposed by Cha et al. (1999). Our studies confirm that the S4 in domain IV is the last voltage sensor to move during repolarization after fast inactivation, and that it contributes $\sim$30% to the total OFF charge. The results in this study demonstrate that the slow movement of the S4 in domain IV during repolarization is intrinsic to the voltage sensor, and not dependent on the binding of the inactivation lid. In the model proposed by Cha el al. (1999), the rate-limiting step during repolarization was proposed to be the unbinding of the inactivation lid. If that were the case, then one would expect either no slow component in the OFF charge of ICM-hH1a$_{MTSET}$ or a component that was intermediate between the fast and slow components of wild-type hH1a. But this was not what was found; the time course of the slow component in the OFF charge in ICM-hH1a$_{MTSET}$ had the same time course as that of $I_{Na}$ inactivation. This finding suggests that the rate-limiting step is not the unbinding of the inactivation lid, but the movement of the S4 in domain IV. However, binding of the inactivation lid did modulate the movement of an additional voltage sensor that contributed 22% to the OFF charge; i.e., the difference between the 53% of charge immobilized in wild-type hH1a and the 31% of charge immobilized in ICM-hH1a$_{MTSET}$ that could be attributed to the S4 in domain IV. Our data taken together with the data of Cha et al. (1999) suggest that a likely candidate for this is the S4 in domain III. When the inactivation lid is not bound to its receptor, either because the inactivation lid has been altered, as in ICM-hH1a$_{MTSET}$, or because the receptor for the inactivation lid has been modified by inhibition of the movement of the domain IV–S4 by site-3 toxins in wild-type hH1a, the S4 in domain III moves rapidly and contributes to the fast component of OFF charge.

We thank WenQing Yu for her excellent technical assistance.

This research was supported by National Heart, Lung and Blood Institute grants HL-PO1-20592 (D.A. Hanck and J.W. Kyle) and HL-R01-44630 (M.F. Sheets).

*Submitted: 29 November 1999*
*Revised: 7 March 2000*
*Accepted: 10 March 2000*

## REFERENCES

Armstrong, C.M., and F. Bezanilla. 1977. Inactivation of the sodium channel. II. Gating current experiments. *J. Gen. Physiol.* 70:567–590.

Bennett, P.B., C. Valenzuela, L.Q. Chen, and R.G. Kallen. 1995. On the molecular nature of the lidocaine receptor of cardiac $Na^+$ channels. Modification of block by alterations in the alpha-subunit III–IV interdomain. *Circ. Res.* 77:584–592.

Benzinger, G.R., C.L. Drum, L.Q. Chen, R.G. Kallen, D.A. Hanck, and D. Hanck. 1997. Differences in the binding sites of two site-3 sodium channel toxins. *Pflügers Arch.* 434:742–749.

Benzinger, G.R., J.W. Kyle, K.M. Blumenthal, and D.A. Hanck. 1998. A specific interaction between the cardiac sodium channel and site-3 toxin anthopleurin B. *J. Biol.Chem.* 273:80–84.

Cha, A., P.C. Ruben, A.L. George, Jr., E. Fujimoto, and F. Bezanilla. 1999. Voltage sensors in domains III and IV, but not I and II, are immobilized by $Na^+$ channel fast inactivation. *Neuron.* 22:73–87.

Chahine, M., A.L. George, Jr., M. Zhou, S. Ji, W. Sun, R.L. Barchi, and R. Horn. 1994. Sodium channel mutations in paramyotonia congenita uncouple inactivation from activation. *Neuron.* 12:281–294.

Chahine, M., I. Deschenes, E. Trottier, L.Q. Chen, and R.G. Kallen. 1997. Restoration of fast inactivation in an inactivation-defective human heart sodium channel by the cysteine modifying reagent benzyl-MTS: analysis of IFM-ICM mutation. *Biochem. Biophys. Res. Commun.* 233:606–610.

Chen, L.Q., V. Santarelli, R. Horn, and R.G. Kallen. 1996. A unique role for the S4 segment of domain 4 in the inactivation of sodium channels. *J. Gen. Physiol.* 108:549–556.

Clarkson, C. 1990. Modification of Na channel inactivation by alpha-chymotrypsin in single cardiac myocytes. *Pflügers Arch.* 417: 48–57.

Featherstone, D.E., J.E. Richmond, and P.C. Ruben. 1996. Interac-

tion between fast and slow inactivation in Skm1 sodium channels. *Biophys. J.* 71:3098–3109.

Greeff, N.G., R.D. Keynes, and D.F. VanHelden. 1982. Fractionation of the asymmetry current in the squid giant axon into inactivating and non-inactivating components. *Proc. R. Soc. Lond. B Biol. Sci.* 215:375–389.

Hanck, D.A., M.F. Sheets, and H.A. Fozzard. 1990. Gating currents associated with Na channels in canine cardiac Purkinje cells. *J. Gen. Physiol.* 95:439–457.

Hanck, D.A., and M.F. Sheets. 1992. Time-dependent changes in kinetics of Na current in single canine cardiac Purkinje cells. *Am. J. Physiol. Heart Circ. Physiol.* 262:H1197–H1207.

Hanck, D.A., and M.F. Sheets. 1995. Modification of inactivation in cardiac sodium channels: ionic current studies with Anthopleurin-A toxin. *J. Gen. Physiol.* 106:601–616.

Hartmann, H.A., A.A. Tiedeman, S.F. Chen, A.M. Brown, and G.E. Kirsch. 1994. Effects of III–IV linker mutations on human heart $Na^+$ channel inactivation gating. *Circ. Res.* 75:114–122.

Higuchi, R., B. Krummel, and R.K. Saiki. 1988. A general method of in vitro preparation and specific mutagenesis of DNA fragments: study of protein and DNA interactions. *Nucleic Acids Res.* 16:7351–7367.

Ho, S.N., H.D. Hunt, R.M. Horton, J.K. Pullen, and L.R. Pease. 1989. Site-directed mutagenesis by overlap extension using the polymerase chain reaction. *Gene.* 77:51–59.

Kellenberger, S., T. Scheuer, and W.A. Catterall. 1996. Movement of the $Na^+$ channel inactivation gate during inactivation. *J. Biol. Chem.* 271:30971–30979.

Khera, P.K., G.R. Benzinger, G. Lipkind, C.L. Drum, D.A. Hanck, and K.M. Blumenthal. 1995. Multiple cationic residues of Anthopleurin B that determine high affinity and channel isoform discrimination. *Biochemistry.* 34:8533–8541.

Khodakhah, K., A. Melishchuk, and C.M. Armstrong. 1998. Charge immobilization caused by modification of internal cysteines in squid Na channels. *Biophys. J.* 75:2821–2829.

Kontis, K.J., A. Rounaghi, and A.L. Goldin. 1997. Sodium channel activation gating is affected by substitutions of voltage sensor positive charges in all four domains [published erratum appears in *J. Gen. Physiol.* 1997. 110:763]. *J. Gen. Physiol.* 110:391–401.

Kuhn, F.J., and N.G. Greeff. 1999. Movement of voltage sensor S4 in domain 4 is tightly coupled to sodium channel fast inactivation and gating charge immobilization. *J. Gen. Physiol.* 114:167–183.

Meves, H., and W. Vogel. 1977. Inactivation of the asymmetrical displacement current in giant axons of *Loligo forbesi*. *J. Physiol.* 267: 377–393.

Neumcke, B., W. Schwarz, and R. Stampfli. 1985. Comparison of the effects of Anemonia toxin II on sodium and gating currents in frog myelinated nerve. *Biochim. Biophys. Acta.* 814:111–119.

Noda, M., S. Shimizu, T. Tanabe, T. Takai, T. Kayano, T. Ikeda, H. Takahashi, H. Nakayama, Y. Kanaoka, N. Minamino, et al. 1984. Primary structure of *Electrophorus electricus* sodium channel deduced from cDNA sequence. *Nature.* 312:121–127.

Nonner, W. 1980. Relations between the inactivation of sodium channels and the immobilization of gating charge in frog myelinated nerve. *J. Physiol.* 299:573–603.

Provencher, S.W. 1976. A Fourier method for the analysis of exponential decay curves. *Biophys. J.* 16:27–41.

Rogers, J.C., Y. Qu, T.N. Tanada, T. Scheuer, and W.A. Catterall. 1996. Molecular determinants of high affinity binding of alpha-scorpion toxin and sea anemone toxin in the S3–S4 extracellular loop in domain IV of the $Na^+$ channel alpha subunit. *J. Biol.Chem.* 271:15950–15962.

Satin, J., J.T. Limberis, J.W. Kyle, R.B. Rogart, and H.A. Fozzard. 1994. The saxitoxin / tetrodoxin binding site on cloned rat brain IIa Na channel is in the electric field. *Biophys. J.* 67:1007–1014.

Sheets, M.F., and D.A. Hanck. 1995. Voltage-dependent open-state inactivation of cardiac sodium channels: gating currents studies with Anthopleurin-A toxin. *J. Gen. Physiol.* 106:617–640.

Sheets, M.F., J.W. Kyle, S. Krueger, and D.A. Hanck. 1996. Optimization of a mammalian expression system for the measurement of sodium channel gating currents. *Am. J. Physiol. Cell Physiol.* 271: C1001–C1006.

Sheets, M.F., and D.A. Hanck. 1999. Gating of skeletal and cardiac muscle sodium channels in mammalian cells. *J. Physiol.* 514:425–436.

Sheets, M.F., J.W. Kyle, R.G. Kallen, and D.A. Hanck. 1999. The Na channel voltage sensor associated with inactivation is localized to the external charged residues of domain IV, S4. *Biophys. J.* 77: 747–757.

Smith, M.R., and A.L. Goldin. 1997. Interaction between the sodium channel inactivation linker and domain III S4–S5. *Biophys. J.* 73:1885–1895.

Starkus, J.G., B.D. Fellmeth, and M.D. Raynor. 1981. Gating currents in the intact crayfish giant axon. *Biophys. J.* 35:521–533.

Stühmer, W., F. Conti, H. Suzuki, X.D. Wang, M. Noda, N. Yahagi, H. Kubo, and S. Numa. 1989. Structural parts involved in activation and inactivation of the sodium channel. *Nature.* 339:597–603.

Thomsen, W.J., and W.A. Catterall. 1989. Localization of the receptor site for alpha-scorpion toxins by antibody mapping: implications for sodium channel topology. *Proc. Natl. Acad. Sci. USA.* 86: 10161–10165.

Vassilev, P.M., T. Scheuer, and W.A. Catterall. 1988. Identification of an intracellular peptide segment involved in sodium channel inactivation. *Science.* 241:1658–1661.

Vedantham, V., and S.C. Cannon. 1998. Slow inactivation does not affect movement of the fast inactivation gate in voltage-gated $Na^+$ channels. *J. Gen. Physiol.* 111:83–93.

West, J.W., D.E. Patton, T. Scheuer, Y. Wang, A.L. Goldin, and W.A. Catterall. 1992. A cluster of hydrophobic amino acid residues required for fast Na{++}-channel inactivation. *Proc. Natl. Acad. Sci. USA.* 89:10910–10914.

Yang, N., and R. Horn. 1995. Evidence for voltage-dependent S4 movement in sodium channels. *Neuron.* 15:213–218.

Yang, N.B., A.L. George, Jr., and R. Horn. 1996. Molecular basis of charge movement in voltage-gated sodium channels. *Neuron.* 16: 113–122.